

DT# 45190
QA: NA
09/08/2005

Submitted to *Proceedings of Migration 2005 in Radiochimica Acta*

Deadline: August 15, 2005

MOL.20051025.0209

**The fate of the epsilon phase in the UO₂ of the Oklo natural fission
reactors**

By Satoshi Utsunomiya^{1,*} and Rodney C. Ewing^{1,2,3}

¹ Department of Geological Sciences, ² Department of Nuclear Engineering &
Radiological Sciences, ³ Department of Materials Science and Engineering, University of
Michigan

*Author for correspondence (E-mail: utu@umich.edu)

Summary. In spent nuclear fuel (SNF), the micron- to nano-sized epsilon phase (Mo-Ru-Pd-Tc-Rh) is an important host of ^{99}Tc which has a long half life (2.13×10^5 years) and can be an important contributor to dose in safety assessments of nuclear waste repositories. In order to examine the occurrence and the fate of the epsilon phase during the corrosion of SNF over long time periods, samples of uraninite from the Oklo natural reactors (~ 2.0 Ga) have been investigated using transmission electron microscopy (TEM). Because essentially all of the ^{99}Tc has decayed to ^{99}Ru , this study focuses on $4d$ -elements of the epsilon phase. Samples were obtained from the research collection at University of Michigan representing reactor zone (RZ) 10 (836, 819, 687) and from RZ 13 (864, 910).

Several phases with $4d$ -metals have been identified within UO_2 matrix at the scale of 50-700 nm; froodite, PdBi_2 , with trace amounts of As, Fe, and Te, and palladodymite or rhodarsenide, $(\text{Pd,Rh})_2\text{As}$. The most abundant $4d$ -metal phase is ruthenarsenite, $(\text{Ru,Ni})\text{As}$, which has a representative composition: As, 59.9; Co, 2.5; Ni, 5.2; Ru, 18.6; Rh, 8.4; Pd, 3.1; Sb, 2.4 in atomic%. Ruthenarsenite nanoparticles are typically surrounded by Pb-rich domains, galena in most cases; whereas, some particles reveal a complexly zoned composition within the grain, such as a Pb-rich domain at the core and enrichment of Ni, Co, and As at the rim.

Some ruthenarsenites and Rh-Bi-particles are embedded in surrounding alteration products, e.g., chlorite, adjacent to uraninite (no further than $\sim 5 \mu\text{m}$). A few of those particles are still coated by a Pb-rich layer. Based on these results, the history that epsilon phases have experienced can be described as follows: (i) The original epsilon phase was changed to, in most cases, ruthenarsenite, by As-rich fluids with other trace metals. Dissolution and a simultaneous precipitation may be responsible for the phase

change. (ii) All Mo and most of the Tc were released from the epsilon phase. Galena precipitated surrounding the 4d-metal phases. (iii) Once the uraninite matrix has dissolved, the epsilon nanoparticles were released and “captured” within alteration phases that are immediately adjacent to the uraninite.

Introduction

Spent nuclear fuel (SNF) consists of >95 wt% of U and contains ~1 wt% of Pu, ~2-3 wt% of the fission products, and other transuranic elements depending on the burn-up [1].

Speciation of the fission products are generally of four types: (i) fission gases and volatiles, (ii) fission products as metals, including Mo, Tc, Ru, Rh, Pd, Ag, Cd, In, Sn, Sb, and Te, (iii) fission products as oxides, including Rb, Cs, Ba, Zr, Nb, Mo, and Te, (iv) fission products dissolved as oxides in the fuel matrix, including Sr, Zr, Nb, and REE [1, 2]. Among these elements, ⁹⁹Tc is one of the elements of greatest concern, because it has a long half life (2.13×10^5 years) and can be an important contributor to the calculated dose after long times in safety assessments of nuclear waste repositories. In addition, Tc is predominantly present as soluble TcO_4^- under oxidizing conditions over wide range of pH (4-10), weakly adsorbed onto mineral surfaces, and unlikely to be incorporated into secondary precipitated uranyl-minerals [3].

In SNF, the micron- to submicron-sized epsilon phase (Mo-Ru-Pd-Tc-Rh) is a major host of Tc. The epsilon-phase structure is hexagonal close packing [2]. The size and composition of epsilon particles vary depending on the fission yield [1, 2, 4]. The first TEM observation of the epsilon phase in LWR (light-water reactor) SNF was by Thomas and Guenther [5], which showed that the epsilon particles occur at ternary grain

boundaries of the uraninite matrix associated with Xe-Kr phase and consist of 40 wt% of Mo, 30 wt% of Ru, 10 wt% of Tc, 15 wt% of Pd and 5 wt% of Rh.

Because the epsilon phase is a main host for Tc, the corrosion behavior has also been examined in a number of previous investigations. Finn et al. [6] reported that under the oxidizing conditions the UO_2 matrix dissolves rapidly, and the epsilon particles remain outside of the altered matrix, indicating relatively slower leach rate of the epsilon particles. The corroded epsilon particles also showed selective leaching of Mo among the five metals [4]. A corrosion test of epsilon particle using Re as a surrogate for Tc also showed a preferential leaching of Mo followed by Re and a precipitation of secondary products containing Mo and Re [7]. Well-controlled dissolution experiments were conducted both under oxic and anoxic conditions by Cui et al. [8, 9]. There are two important aspects in the corrosion behavior: (i) The leach rate of the metals is in the order of: (fast) $Mo > Tc > Ru \sim Rh \sim Pd$ (slow). The leach rate of Mo, under reducing conditions, is estimated to be 1.5×10^{-7} g/cm²/day which is ~40 times faster than that of Tc and 10^3 - 10^4 times faster than the other $4d$ -metals. (ii) The leach rate of the ϵ -phase under oxidizing condition is ~100 times faster than that under reducing condition [8, 9].

In the natural fission reactors at Oklo, Gabon, $4d$ -metal phases have been found in the reactor zones (RZ) 10 and 13 [10-13]. The phases were inferred to be ruthenarsenite, RuAs, or ruasite, RuAsS, based only on their chemistries. In addition, the occurrence of the $4d$ metals in these previous studies is very different from the epsilon particles observed in SNF: The particle size is from 5 nm to a few micrometers in SNF [4]; whereas, the $4d$ metal phases in the previous studies on Oklo showed a sporadic occurrence at the size of 50-100 μm [10, 11]. Because the Oklo reactors are 2.0 billion

years old, which is much longer than the half-life of Tc (2.13×10^5 years), essentially all of the ^{99}Tc has decayed to ^{99}Ru . Indeed, the Ru isotopic ratio, $^{99}\text{Ru}/^{101}\text{Ru}$, in the *4d* metal phases was ~ 2.3 , which is larger than the ratio of the whole rock, ~ 1.2 , indicating that the Tc was incorporated into the metallic aggregates [11]. In the present study, the *4d* metal phase in uraninite matrix of the Oklo natural fission reactors is investigated in more detail at the nanoscale using the advanced TEM techniques to elucidate fate of the epsilon phases over geologic periods, ~ 2.0 billion years.

Sample description and experimental methods

Uraninite samples used in this study are: #836, #819, and #687 from reactor zone (RZ)-10; #864 and #910 from RZ-13, #943 from Okélobondo. Sample numbers refer to the research collection at the University of Michigan. These samples were selected because previous studies [10-13] reported the presence of trace Ru-phase in RZ-10 and -13. No Ru-phase was observed in #943 from Okélobondo.

Back-scattered electron (BSE) imaging was performed using scanning electron microscopy (SEM), HITACHI S3200, with an accelerating voltage of 15 kV. High-resolution transmission electron microscopy (HRTEM) and high-angle annular dark-field scanning transmission electron microscopy (HAADF-STEM) with energy dispersive X-ray spectrometry (EDS) were completed using a JEOL 2010F. The detailed procedure of HAADF-STEM has previously been described in Utsunomiya and Ewing [14]. In general, contrast in HAADF-STEM correlates to mass, density, periodicity of atoms and sample thickness [15], and the major advantage is that the contrast does not change significantly near the focal point due to the incoherent imaging process [16]. In the

present samples, the epsilon phase is lighter than the matrix uraninite, and shows darker contrast than uraninite. The TEM specimens were prepared by polishing to a thickness of a few tens of μm , followed by ion milling (GATAN PIPS) using 4.0 kV Ar ions.

Results and discussion

In #819, a Ru-As particle ~ 300 nm in size was identified surrounded by a Pb-rich region within the uraninite matrix (Fig. 1a). The composition of the particle was determined semi-quantitatively as: As, 59.9; Co, 2.5; Ni, 5.2; Ru, 18.6; Th, 8.4; Pd, 3.1; Sb, 2.4 in atomic% (Fig. 1b). The Ru-As phase was not a single particle, but an aggregate of 100-200 nm sized particles. The phase was identified as ruthenarsenite, $(\text{Ru,Ni})\text{As}$, based on the HRTEM image and the FFT (fast Fourier transformed) image (Fig. 1c). Another Ru-phase observed in this sample is at the size of 600-700 nm. The elemental distribution is rather complicated for this inclusion as shown in the elemental maps (Fig. 1a). Lead occurs at the core of the particle; whereas, the rim of the inclusion consists of Ni, Co, and As without Ru. The Ru is enriched in the intermediate zone, associated with As and Ni, forming ruthenarsenite. This complexly mixed texture suggests that a process of dissolution and precipitation occurred within this inclusion.

In #864, a Bi-Pd particle was observed at the size of 40-60 nm surrounded by an amorphous Pb-rich region (Fig. 2a). Semi-quantitative analysis based on EDX spectrum gave: As, 6.4; Fe, 2.4; Pb, 22.8; Bi, 28.0; Pd, 35.7; Te, 4.7 in atomic %. There are three possible minerals inferred from this composition: froodite, PdBi_2 ; urvantsevite, $\text{Pd}(\text{Bi}, \text{Pb})_2$; and polarite, $\text{Pd}(\text{Bi}, \text{Pb})$. The FFT image (the inset) was indexed using the crystallographic information of froodite. The indices are possible diffraction maxima of

froodite; whereas, the other two minerals give indices that were not possible diffraction maxima or a lower indexed zone axis. Thus, this phase has the froodite structure and possibly some Pb atoms and the other trace metals have substituted for Bi.

In #836, a Mo-particle was observed embedded in a Pb-inclusion, galena. The Pb-inclusion is about 200 nm in the size, and the Mo-rich area is limited to <50 nm (Fig. 2b). The EDS analysis indicates the presence of Mo and Pb (+S), and U peaks are excited signals from surrounding uraninite. Because there is no pure Mo+Pb phase in nature, and Pb occurs as sulfide, Mo is inferred to be a Mo-sulfide. The second particle observed in #836 is a Ru-rich particle of ~400 nm in size (Fig. 2c). The STEM image and the elemental map clearly show that Pb-rich region (galena) surrounds the Ru-particle. The semi-quantitative analysis gave: As, 44.0; Fe, 1.1; Co, 1.3; Ni, 6.3; Ru, 37.1; Rh, 4.1; Pd, 2.0; Sb, 1.5; Te, 2.5 in atomic%. The particle is most likely ruthenarsenite, based on the similar composition to the particle found in #819. The third particle in #836 is an elongated Ru-rich particle surrounded by a Pb-rich domain, which has two phases within the particle: Ru-As-rich region and Pd-Rh-rich region (Fig. 2d). Semi-quantitative analysis gave: As, 16.0; Ru, 5.8; Rh, 26.7; Pd, 39.2; Sn, 2.8; Sb, 9.4 in atomic%. Because there are a limited number of Pd-Rh minerals in nature, the phase is either palladodymite or rhodarsenide, both of which have a chemical formula of $(\text{Pd, Rh})_2\text{As}$. The Ru-As-rich region at the edge of the particle was identified as ruthenarsenide.

In #687, a Ru-As-particle, most likely ruthenarsenite, is present, ~50 nm in size, surrounded by a Pb-matrix (Fig. 2e). The EDS analysis gave: As, 40.4; Fe, 1.1; Ni, 2.9; Ru, 46.9; Th, 5.2; Sb, 3.6 in atomic%.

In #910, the only particle that consists of *4d*-elements was observed in a galena matrix, not in uraninite and the other clay minerals (Fig. 2f), indicating that the Rh,Pd-particle can also be transported by Pb-rich fluids.

Summarizing the observations, Ru-phases are associated with a Pb-phase, in most cases, galena. The galena may precipitate in the space created by dissolution of the epsilon particles. On the other hand, the texture of the void space where galena has precipitated is similar to that of the fission gas bubbles surrounding the epsilon particles [5, 17]. Thus, it may be that the void spaces between the UO₂ matrix and Ru-particles is originally filled by the fission gases and replaced by precipitates from Pb-rich fluids later. Although there is a wide range in the variation of the composition of the Ru-phase, representative compositions (Fig. 3) reveal that a large amount of As and the other trace metals were added to the epsilon particle; whereas, Mo is leached out, and Tc has been decayed to Ru or dissolved as well. The selective leaching of Mo and Tc from an epsilon phase is consistent with the previous studies of the dissolution of the epsilon phase [8, 9]. The particles observed in the present study are 50-700 nm in size, which is much smaller than the sizes previously reported, 50-100 μm [10], and the occurrence and texture in the sample studied appear to be similar to the epsilon phases in SNF. The *4d* metal phases found in [10] may have formed by the precipitation of released Tc and the other *4d*-metals.

Some ruthenarsenite particles are embedded in surrounding secondary alteration products, chlorite, in most cases (Fig. 4a). A few grains have even retained the Pb-rich coating, which is most likely galena (Fig. 4b). In addition, these ruthenarsenite nanoparticles are observed only immediately adjacent to the uraninite (Fig. 4c and d).

This suggests that the ruthenarsenites nanoparticles, although colloid-sized, may not be transported more than several μm , probably due to their high density.

The history which the epsilon phase has experienced in Oklo's reducing environment can be described as the follows: (i) The epsilon phases were influenced by As-bearing fluids with the other trace metals. Both Mo and Tc were leached out, or most Tc decayed to Ru within the epsilon phases. (ii) Additionally the entire grain may dissolve with the simultaneous precipitation of ruthenarsenite. (iii) A certain fraction of precipitated ruthenarsenite was subsequently dissolved, and the particle size became smaller. Lead-rich fluids were introduced and galena precipitated filling the space between epsilon particles and the uraninite matrix. Fission gases may occur initially surrounding the epsilon particles, and this provided void space for the formation of precipitates from the Pb-bearing fluids. (iv) Once the uraninite matrix was altered and the ruthenarsenite nanoparticles were released, the colloid-sized epsilon particles did not appear to travel more than several microns from the original host uraninite.

References

1. Oversby, V. M.: Nuclear waste materials. In: *Material science and technology: a comprehensive treatment, Nuclear Materials*. **10B** (Frost, B. R. T., ed.) VCH. Weinheim, Germany (1994) pp. 392-442.
2. Kleykamp, H.: The chemical state of fission products in oxide fuels. *J. Nucl. Mater.* **131**, 463 (1985).
3. Chen, F., Burns, P. C., Ewing, R. C.: Near-field behavior of ⁹⁹Tc during the oxidative alteration of spent nuclear fuel. *J. Nucl. Mater.* **278**, 225 (2000).
4. Buck, E. C., Hanson, B. D., McNamara, B. K.: The geochemical behavior of Tc, Np and Pu in spent nuclear fuel in an oxidizing environment. In: *Energy, Waste, and the Environment: a Geochemical Perspective*. (Gieré, R. and Stille, P., eds.) Geological Society, London, Special Publication, **236**, pp. 65-88.
5. Thomas, L. E., Guenther, R. J.: Characterization of low-gas release LWR fuels by transmission electron microscopy. In: *Scientific Basis for Nuclear Waste Management XII*. (Lutze, W., Ewing, R. C., eds.) Mater. Res. Soc. Symp. Proc. **127**, 293 (1989).
6. Finn, P. A., Hoh, J. C., Wolf, S. F., Surchik, M. T., Buck, E. C., Bates, J. K.: Spent nuclear fuel reaction – the behavior of the ε-phase over 3.1 years. In: *Scientific Basis for Nuclear Waste Management XX*. (Gray, W. J., Triay, I. R., eds.) Mater. Res. Soc. Symp. Proc. **465**, 527 (1997).
7. Wronkiewicz, D. J., Watkins, C. S., Baughman, A. C., Miller, F. S., Wolf, S. F.: Corrosion testing of a simulated five-metal epsilon particle in spent nuclear fuel. In:

- Scientific Basis for Nuclear Waste Management XXV.* (McGrail, B. P., Cragnolino, G. A., eds.) Mater. Res. Soc. Symp. Proc. **713**, 625 (2002).
8. Cui, D., Eriksen, T., Eklund, U. B.: On metal aggregates in spent fuel, synthesis and leaching of Mo-Ru-Pd-Rh Alloy. In: *Scientific Basis for Nuclear Waste Management XXIV.* (Hart, K. P., Lumpkin, G. R., eds.) Mater. Res. Soc. Symp. Proc. **663**, 427 (2001).
 9. Cui, D., Low, J., Sjöstedt, C. J., Spahiu, K.: On Mo-Ru-Tc-Pd-Rh-Te alloy particles extracted from spent fuel and their leaching behavior under Ar and H₂ atmosphere. *Radiochim. Acta* **93**, 265 (2005).
 10. Gauthier-Lafaye, F., Holliger, P., Blanc, P.-L.: Natural fission reactors in the Franceville basin, Gabon: A review of the conditions and results of a “critical event” in a geologic system. *Geochim. Cosmochim. Acta* **60**, 4831 (1996).
 11. Hidaka, H., Holliger, P.: Geochemical and neutronic characteristics of the natural fossil fission reactors at Oklo and Bangombé, Gabon. *Geochim. Cosmochim. Acta* **62**, 89 (1998).
 12. Janeczek, J.: Mineralogy and geochemistry of natural fission reactors in Gabon. In: *Uranium: Mineralogy, Geochemistry, and the Environment.* (Burns, P. C., Finch, R. J., eds.) Mineralogical Society of America, Washington, D. C. (1999) p.321.
 13. Jensen, K. A., Ewing, R. C.: The Okélobondo natural fission reactor, southeast Gabon: Geology, mineralogy, and retardation of nuclear-reaction products. *GSA Bulletin* **113**, 32 (2001).
 14. Utsunomiya, S., Ewing, R. C.: Application of high-angle annular dark field scanning transmission electron microscopy, scanning transmission electron microscopy-energy

dispersive X-ray spectrometry, and energy-filtered transmission electron microscopy to the characterization of nanoparticles in the environment. *Environ. Sci. Technol.* **37**, 786 (2003).

15. Utsunomiya, S., Yudintsev, S., Ewing, R. C.: Radiation effects in ferrate garnet. *J. Nucl. Mater.* **336**, 251 (2005).
16. Pennycook, S. J., Jesson, D. E.: High-resolution incoherent imaging of crystals. *Phys. Rev. Lett.* **64**, 938 (1990).
17. Ray, I. L. F., Thiele, H., and Matzke, H.: Transmission electron microscopy study of fission product behavior in high burnup UO₂. *J. Nucl. Mater.* **188**, 90 (1992).

Figure caption

Fig. 1. (a) HAADF-STEM image of a Ru-particle found in #819 associated with the elemental maps of the square region. (b) The EDS profile and (c) HRTEM image of the Ru-particle. (d) HAADF-STEM image of the other Ru-phase showing a complex chemical zoning.

Fig. 2. HAADF-STEM images of 4*d*-metal particles in the samples; (a) #864, (b-d) #836, (e) #687, and (f) #910, associated with the elemental maps of the square region. The inset in (a) is a FFT image of the Bi-Pd-particle, which is identified to be froodite, PdBi₂. An EDS profile of the point indicated by the arrow is inserted in (b).

Fig. 3. Representative compositions of 4*d*-metal phases by semi-quantitative EDS analysis. The composition of epsilon phase in SNF [5] is also given for the comparison.

Fig. 4. (a) HAADF-STEM image of several ruthenarsenite grains embedded in secondary alteration phase, chlorite. (b) An enlarged HAADF-STEM image with the elemental maps of the square region. (c) Rh-Bi-particles and (d) Ru-particles embedded in the chlorite immediately adjacent to uraninite.

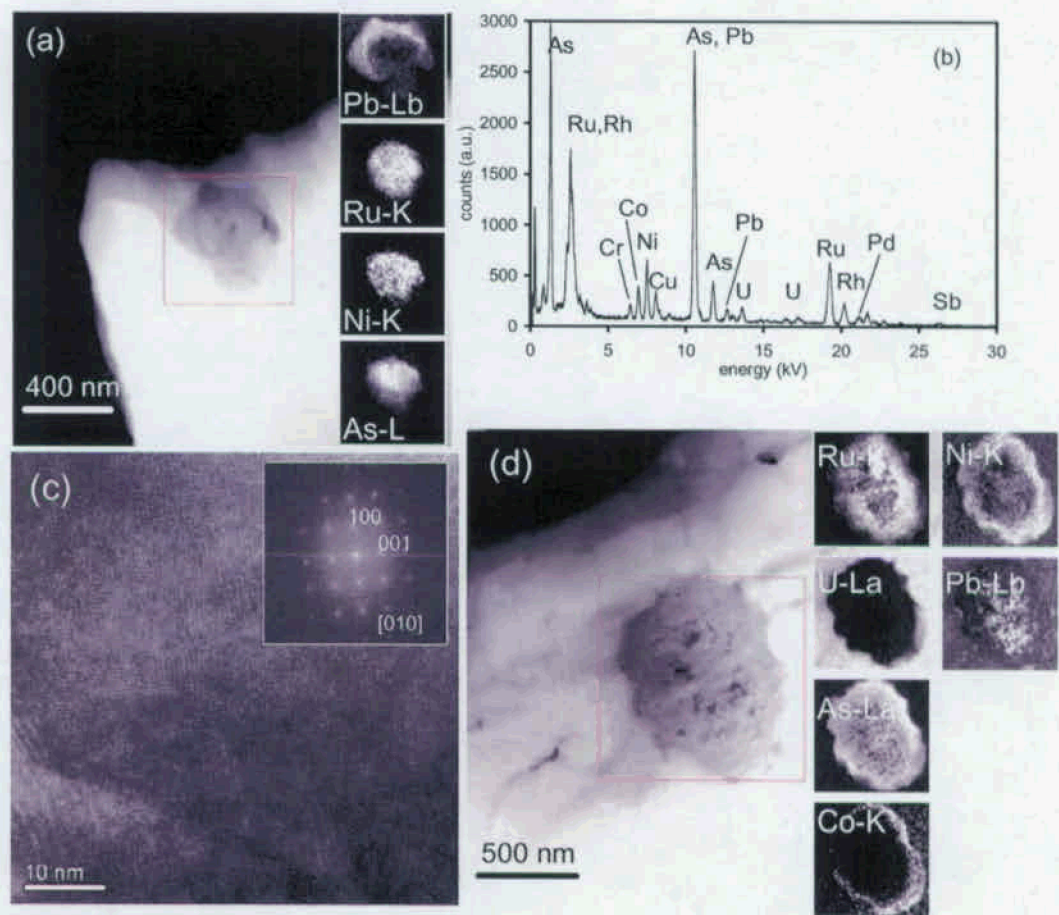


Figure 1

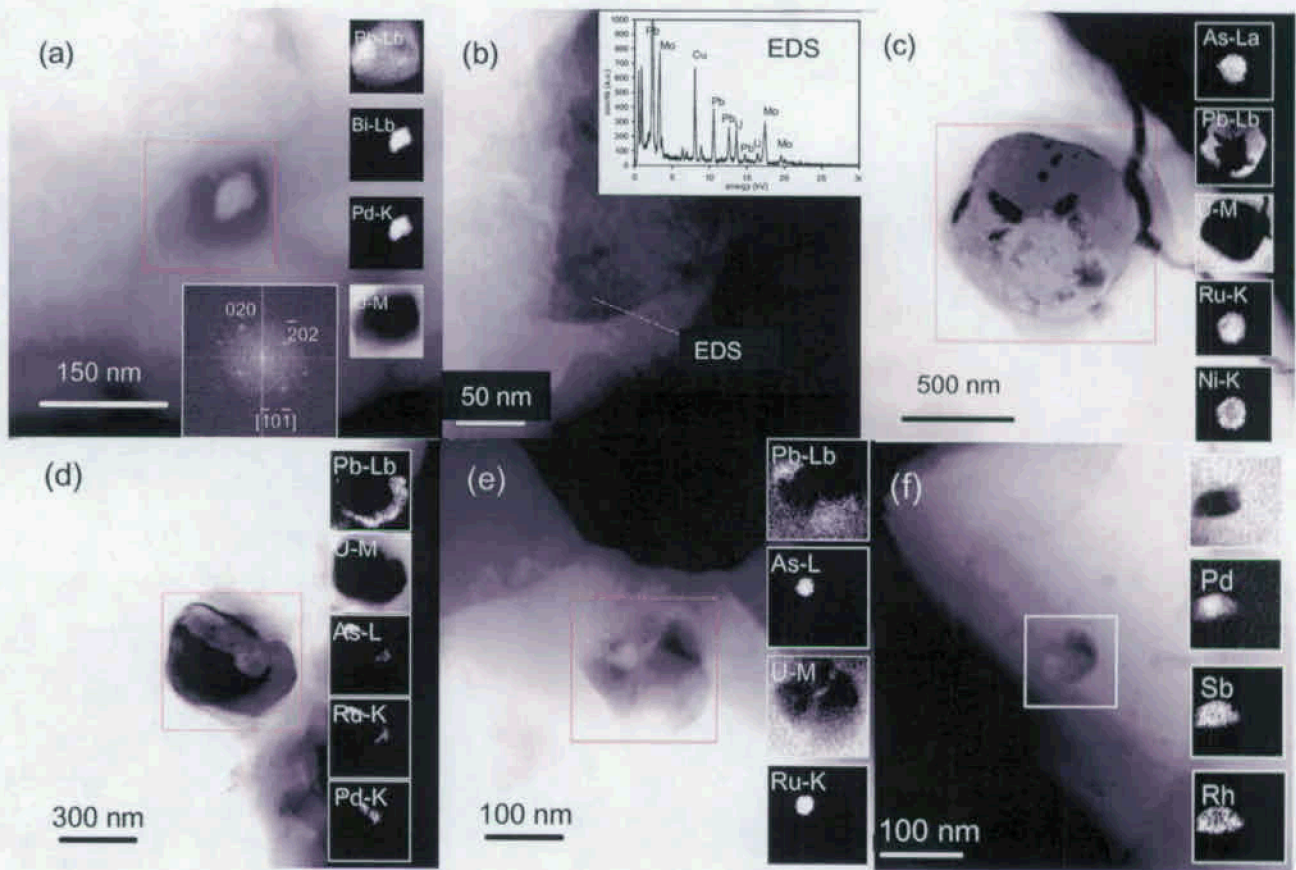


Figure 2

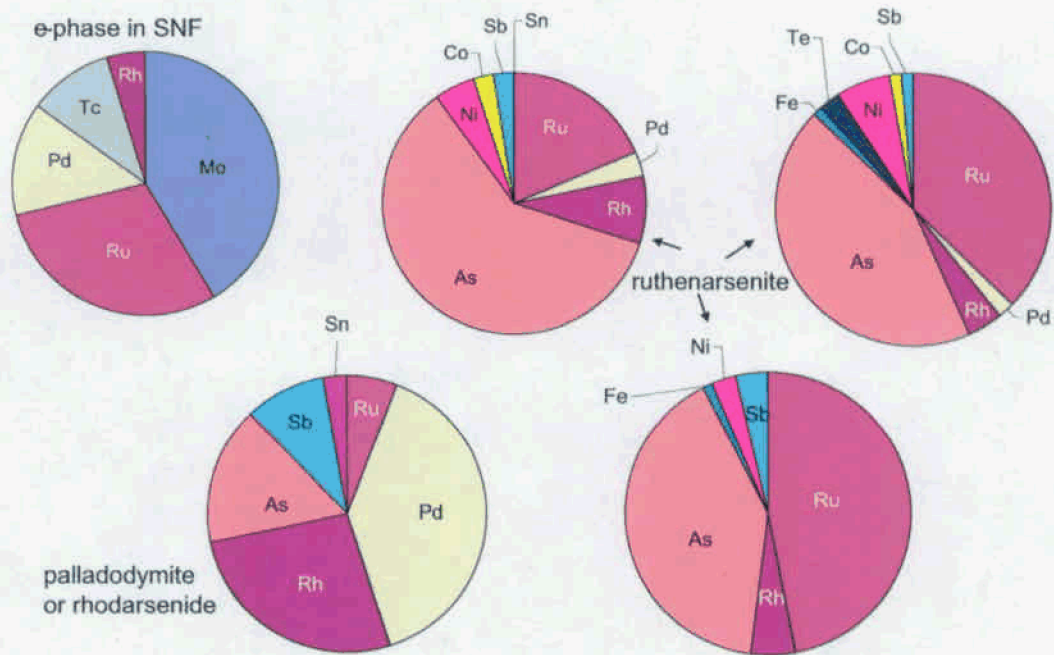


Figure 3

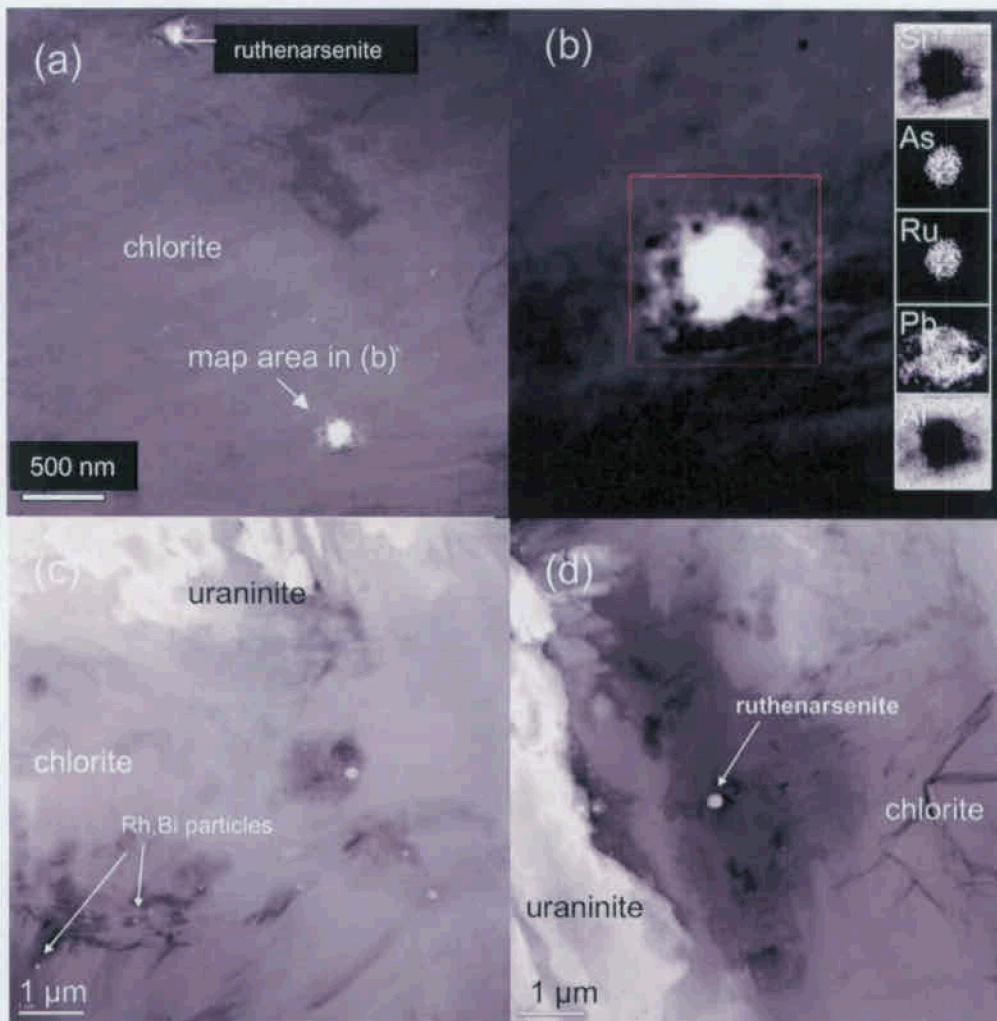


Figure 4